



Nanoemulsification of Essential Oil Blend by Ultrasound: Optimization of Physicochemical, Antioxidant Properties, and Activity Against *Escherichia coli*

Luiz Torres Neto^{1,2,3} · Maria Lucia Guerra Monteiro^{1,2,3,4} · Yhan da Silva Mutz^{1,2,3} · Renata Valeriano Tonon⁵ · Carlos Adam Conte-Junior^{1,2,3,4}

Received: 19 September 2023 / Accepted: 11 December 2023 / Published online: 16 December 2023
© The Author(s), under exclusive licence to Springer Science+Business Media, LLC, part of Springer Nature 2023

Abstract

This study aimed to select the best conditions for producing a nanoemulsion loaded with an essential oil blend (NEOB) to achieve maximum antimicrobial and antioxidant activities. The NEOB consisted of lemongrass (*Cymbopogon citratus*; LEO; 60%) and thyme (*Thymus vulgaris*; TEO; 40%). The effect of ultrasound time exposition at 300 W (5, 18, and 30 min) and essential oil concentration (5, 11, and 20 mg/mL) on these responses was evaluated after obtaining NEOB and after an oxidation assay with UVC-LED exposure. Nanoemulsions were analyzed for their physicochemical and biological properties. Overall, droplet size, zeta potential, minimum inhibitory concentrations (MIC) against *Escherichia coli*, DPPH free radical scavenging activity, and ferric-reducing antioxidant power were affected by essential oil concentration and/or ultrasound time exposition in a non-linear fashion. The NEOB (average size, 68.88 ± 2.84 nm) with 20.5 mg/mL of essential oil and sonicated for 35.7 min achieved the highest anti-*E. coli* (MIC, 0.44 mg/mL) and antioxidant activity (FRAP, 1.17 μ mol TROLOX equivalent/g), remaining stable even after high UVC-LED doses (6.41 J/cm² exposure, $p < 0.05$). This study reveals the promising potential of NEOB obtained from ultrasound for sustainable industrial applications.

Keywords Desirability function · CCRD · *Escherichia coli* · FRAP · Ultraviolet light-emitting diode

Introduction

Essential oils (EOs) have great potential applications in the food industry due to their proven action against food-borne pathogens and antioxidant activity (da Silva, 2023b; Torres Neto et al., 2022). Furthermore, EOs have aroused wide attention mainly due to their cost-effectiveness and sustainability claim, in line with the global need for new and nontoxic preservative agents with antimicrobial and antioxidant properties (Konfo et al., 2023; Lelis et al., 2023).

Despite this potential, EOs show drawbacks for application in the food industry, such as hydrophobicity, volatility, intense flavor, sensitivity to oxygen, light, heat, and oxidability (Haç-Wydro et al., 2017; Yang et al., 2022). Therefore, several studies have proposed the nanoencapsulation of EOs in modified or controlled release systems as an emerging strategy (Delshadi et al., 2020; Mukurumbira et al., 2022; Singh et al., 2023). Indeed, it physically protects the EOs and increases their solubility and surface area, reaching new properties and greater effectiveness (McClements

✉ Luiz Torres Neto
luiztorresneto@ufrj.br

✉ Carlos Adam Conte-Junior
conte@iq.ufrj.br

¹ Center for Food Analysis (NAL), Technological Development Support Laboratory (LADETEC), Cidade Universitária, Rio de Janeiro, RJ 21941-598, Brazil

² Laboratory of Advanced Analysis in Biochemistry and Molecular Biology (LAABBM), Department of Biochemistry, Federal University of Rio de Janeiro (UFRJ), Cidade Universitária, Rio de Janeiro, RJ 21941-909, Brazil

³ Graduate Program in Food Science (PPGCAL), Institute of Chemistry (IQ), Federal University of Rio de Janeiro (UFRJ), Cidade Universitária, Rio de Janeiro, RJ 21941-909, Brazil

⁴ Graduate Program in Veterinary Hygiene (PPGHV), Faculty of Veterinary Medicine, Fluminense Federal University (UFF), Vital Brazil Filho, Niterói, RJ 24220-000, Brazil

⁵ Embrapa Agroindústria de Alimentos, Av. das Américas, Rio de Janeiro, RJ 2950123020-470, Brazil

et al., 2021). Furthermore, the utilization of EOs in various encapsulation systems (e.g., nanoemulsions, nanocapsules, liposomes) represents an approach that has already demonstrated its efficacy in enhancing food matrices' quality, safety, and shelf-life (Ribeiro et al., 2021; Wang et al., 2023).

An oil-in-water nanoemulsion is a colloidal system formed by dispersing one liquid in another immiscible liquid using an appropriate emulsifier (Gupta et al., 2016). It is characterized by small droplet sizes (< 200 nm) and high surface-to-volume ratios, besides being easy to produce, and thus a promising candidate for the efficient delivery of lipophilic bioactive compounds (McClements, 2012; McClements et al., 2021). Different techniques can be applied to achieve a nanometric size, such as high-pressure homogenization, microfluidization, and ultrasound (da Silva, et al., 2023a). These methods are based on mechanical devices generating disruptive forces needed for droplet breakdown (high-energy techniques; Abbas et al., 2013). However, adjusting the different variables of these techniques is necessary to ensure stable nanoemulsions, with low polydispersity (PDI) and high zeta potential values without compromising or even improving the EO biological activity, thus enabling their industrial application into foods.

The ultrasound technique has high acceptability due to its efficiency, low cost, and better control of variable systems (Khatkar et al., 2018). Its mechanism is based on the phenomenon of acoustic cavitation that generates pressure fluctuations, creating localized turbulence, thereby reducing the droplet size by rupture (Alves de Aguilar Bernardo et al., 2023), and the ultrasound mechanisms may influence the nanometric system polydispersion and its charge (Yang et al., 2022). Therefore, different final nanoemulsion properties can be obtained by modifying processing parameters (e.g., oil to surfactant ratio, oil and surfactant types, ultrasound exposure time, and ultrasound power; Teng et al., 2020).

Obtaining an essential oil blend (EOB) is a promising emerging approach to optimizing the antioxidant and antimicrobial activity of the EOs (Baj et al., 2023; Crespo et al., 2019; Fadil et al., 2018; Ouedrhiri et al., 2016). Moreover, no studies optimize nanoemulsions (NEs) for carrying EOB, where existing studies are limited to optimizing (da Silva, 2023b; Yang et al., 2022) or obtaining NEs for individual EOs (Hasheminya & Dehghannya, 2022; Hemmatkhan et al., 2020; Salvia-Trujillo et al., 2013). Indeed, these studies have reached successful stable NEs (e.g., diameter, low PDI, and high zeta values); nevertheless, the influence of obtaining NEs on biological activity is limited only to antimicrobial activity. The NE optimization for transporting an antioxidant and antimicrobial EOB and studying the process's impact on biological activity addresses a critical knowledge gap in the literature.

The aromatic oils *Thymus vulgaris* (TEO) and *Cymbopogon citratus* (LEO) have a great single antioxidant activity already documented in the literature (Dinu et al., 2021; Istiqomah et al., 2022; Oun et al., 2022). Furthermore, these two EOs already showed a synergic antibacterial activity being justified by the combination observed in the functional groups present in the EOs, such as phenols (carvacrol and thymol) and aldehydes (geranial and neral), which improve the activity because they are two of the most effective antimicrobial functional groups (Kalemba & Kunicka, 2003; Torres Neto et al., 2022). In this sense, these two EOs are promising in the study of developing optimized antioxidant and antimicrobial blends and an encapsulation system that enhances their effectiveness or maintains their original biological activities.

The development of bioactive NE for food application is an essential demand of the food industry for new natural preservatives, in contrast to synthetic ones. Indeed, the clean label market is projected to reach US\$ 169.024 million by 2033, including a Compound Annual Growth Rate (CAGR) of 16.2% between 2023 and 2033 (Future Market Insights, 2023). Therefore, the study of NEs optimized with EOB is of outstanding contribution to the food industry. Thus, this study aimed to select the best conditions to obtain an NE loaded with an EOB, which was optimized in a previous study, considering the variables EOB concentration and sonication time, to achieve improved physical properties, antioxidant, and anti-*Escherichia coli* activities and an oxidation assay with UVC-LED exposure.

Material and Methods

Material

Lemongrass (*Cymbopogon citratus*; LEO) and thyme (*Thymus vulgaris*; TEO) essential oils were acquired from Quinari® (Ponta Grossa, Brazil). Tween 80 was purchased from Rei-Sol (Rio de Janeiro, Brazil). 2,2-Diphenyl-1-picrylhydrazyl (DPPH), 2,4,6-Tris(2-pyridyl)-s-triazine (TPTZ), and (S)-trolox methyl ether (Trolox) were obtained from Sigma-Aldrich (São Paulo, Brazil).

Experimental Design

The effects of EOB concentration (5, 11, and 20 mg/mL) and ultrasound exposure time (5, 18, and 30 min) on physicochemical and biological characteristics of nanoemulsion essential oil blend (NEOB), including its stability to UVC-LED exposure, were studied. The concentration of surfactant (Tween 80) was fixed at 20 mg/mL. In other words, two main factors were considered to evaluate the physicochemical and biological properties of NEs: (I) different proportions

of EOB to surfactant (Tween 80) and (II) exposure of emulsions to different times (min) in the amplitude of 40% (300 W; variables chosen through prior optimization). Table 1 shows the experimental layout of the 2^2 central composite rotating design (CCRD) generating 11 experiments, including three central point replicates.

Nanoemulsion Preparation

The EOB used in this study was obtained by previous optimization studies evaluating the effect of three EOs (oregano, thyme, and lemongrass) on the antioxidant (DPPH and FRAP) and anti-*Escherichia coli* activities through simplex-centroid mixture design and desirability function (D) using DoE (Statistica v.9.0 software; Stasoft, Tulsa, OK, USA; Supplementary Fig. 1). In this sense, an ideal ratio with maximum antioxidant and anti-*Escherichia coli* activity was obtained using these three EOs (Supplementary Fig. 1). Briefly, the EOB with TEO and LEO (60:40) was used as the oil phase, and the aqueous phase consisted of Tween 80 (20 mg/mL) in ultrapure water (Mili-Q IQ 7005, Merck, Germany). The oil and aqueous phases were mixed and homogenized for 10 min at 13,400 rpm (Ultraturrax, IKA® T10, China) to form a coarse emulsion; the emulsion was subjected to sonication with ultrasound (VC-750 Ultrasonic Processor, 20 kHz, 750 W; Sonics, Materials Inc., Newtown, USA) equipped with 19-mm-diameter probe using an ice bath for temperature control for droplet size reduction.

Nanoemulsion Characterization

Droplet size, Polydispersion, and Zeta Potential (ζ)

The droplet size distribution and the ζ -potential (mV) were determined using the Zetasizer Nano® (Model 590, Malvern

Instruments, UK). Samples were diluted (1:5) in deionized water. The polydispersity was expressed in the polydispersion index (PDI). The size distribution was represented by radar charts (Bianchin et al., 2015) with adaptations for DLS, wherein D_{10} , D_{50} , and D_{90} values (size of 10%, 50%, and 90% of the drops population) of cumulative intensity (Di), volume (Dv), and number (Dn) were used. These analyses were carried out in triplicate.

Antioxidant Activity

DPPH Free Radical Scavenging Activity The 2,2-diphenyl-1-picrylhydrazyl (DPPH) radical reduction capacity was determined according to Rufino et al. (2007) with modifications (Baj et al., 2018). The % of DPPH radical inhibition rate was determined in triplicate by applying the absorbance values (A) in the Eq. 1:

$$\text{Inhibition (\%)} = (A_{\text{control}} - A_{\text{sample}}) / A_{\text{control}} \times 100 \quad (1)$$

Ferric-Reducing Antioxidant Power (FRAP) Assay The ferric ion-reducing capacity was determined in triplicate, as Benzie and Strain (1996) and Rufino et al. (2006) described. The calibration curve was assembled based on the TROLOX pure standard (from 160 to 800 $\mu\text{mol/L}$; $R^2 = 0.9995$), and the results were expressed in $\mu\text{mol TROLOX equivalent/g}$.

Determination of Minimum Inhibitory Concentration (MIC)

The MIC against *Escherichia coli* ATCC 25922 was determined by micro-dilution assay in sterile 96 U-bottom well microplates (OLEN, China), following the methodology of Wiegand et al. (2008). The *E. coli* used in this study was obtained from the culture bank of the Oswaldo Cruz Foundation (FIOCRUZ, Rio de Janeiro, Brazil), where the strain was stored in methylene

Table 1 Independent variables from the central composite rotatable design (CCRD; X_1 and X_2) and ultrasound processing conditions

Treatments ^a	Tween 80 (mg/mL)	EOB (mg/mL) (X_1)	Time (min) (X_2)	Amplitude (%)	Power (W)	U.I. (W/cm ²)	AED (kJ/mL)
1	20.00	5.00	5.00	40	3.11	1.10	18.67
2	20.00	5.00	30.00	40	0.93	0.33	16.74
3	20.00	20.00	5.00	40	4.19	1.48	12.56
4	20.00	20.00	30.00	40	1.86	0.66	33.49
5	20.00	0.40	18.00	40	0.78	0.27	8.37
6	20.00	21.60	18.00	40	1.55	0.55	16.74
7	20.00	11.00	0.32	40	2.16	0.76	0.42
8	20.00	11.00	35.68	40	1.40	0.49	29.30
9	20.00	11.00	18.00	40	2.33	0.82	25.12
10	20.00	11.00	18.00	40	2.33	0.82	25.12
11	20.00	11.00	18.00	40	2.33	0.82	25.12

^aEOB essential oil blend, U.I. ultrasound intensity, AED acoustic density energy

blue eosin (EMB; Kasvi, Spain). A NEOB stock solution of 8 mg/mL in BHI broth with 0.5% Tween 80 was prepared, from which two-fold serial dilutions on the plate were made. Then, 100 μ L of *E. coli* suspension in saline solution with a 6 log CFU/mL concentration was added to the wells. The bacterial suspension was standardized by adjusting its optical density at 1 O.D., resulting in 8 log CFU/mL (confirmed by plating), which was subsequently serially diluted. The final pathogen concentration in the wells was approximately 5.5 log CFU/mL (confirmed by plating). The first well used the stock solution diluted by the pathogen inoculum, resulting in a 4 mg/mL NEOB concentration, which was subsequently twofold diluted up to 0.05 mg/mL in the last well. The microplates were incubated for 24 h at 35 °C, and the MIC value was determined as the lowest NEOB concentration to prevent visible bacterial growth in the plates. A row of wells with only BHI + Tween 80 and *E. coli* was used as a positive control. While a BHI + 0.5% Tween 80 row was left as sterility control.

Stability of NEOB Against UVC-LED Exposure

The NEOBs with different EO concentrations (5, 10, and 20 mg/mL) were exposed to UVC-LED at 1.78 mW/cm² at different times (0, 20, 40, and 60 min), resulting in different doses (0, 2.14, 4.27, and 6.41 J/cm², respectively). The treatments were performed using modules with simultaneous top and bottom illumination with emissions at 275 nm (Black Box Smart®; BioLambda, Sao Paulo, Brazil). The distance between samples and LEDs was 15 cm. After that, the NEOBs were characterized (“Nanoemulsion Characterization” section) in triplicate.

Statistical Analysis and Model Validation

The effects of different proportions of EOB, surfactant, and ultrasound exposure times on the size, zeta potential, antibacterial (*E. coli*), and antioxidant (DPPH and FRAP) activities were assessed by polynomial equation models, considering only the significant terms ($p < 0.05$), and represented by response surface graphs. Lack-of-fit (LOF), adjusted R^2 (R^2_{adj}) value, and mean square error (MSE) were used to evaluate model’s goodness of fit. After the individual modeling, the desirability function was applied to model the MIC and FRAP variables to obtain an optimum nanoemulsion with the maximum anti-*Escherichia coli* and antioxidant conjoint activities. An external validation was performed with the optimal condition determined from the desirability function and two experimental conditions different from those generated from CCRD. Further, observed and predicted values were used to calculate the accuracy factor (Af) and bias factor (Bf) to externally assess the model prediction (Baranyi et al., 1999). Statistica 12® software was used to perform all statistical analyses.

Results and Discussion

Droplet Size and PDI

All treatments reached the nanometer range with sizes < 200 nm (Supplementary Table 1). In general, the size distribution of 90% of the population of drops of cumulative intensity (Di), volume (Dv), and number (Dn) decreased with increasing exposure time (min) and with decreasing EOB concentration non-linearly (Fig. 1A–F; Table 2).

The non-linearity observed in Di can be attributed to “over-processing” (Paniwnyk, 2017; Tan et al., 2016), wherein a long time of sonication exposition can increase the droplet size due to coalescence. On the other hand, low exposure times did not allow for efficient droplet size reduction (e.g., treatments 7; Table 1 and Fig. 1). Moreover, a high EO to Tween ratio could mitigate the US overprocessing effect since it would reduce the free surfactant available to degradation. The EOB and Tween 80 ratio may also greatly influence the size distribution. Excess surfactants treated with ultrasound may form micelles with larger sizes (Yang et al., 2022). Otherwise, the decrease of Tween 80 in relation to EOB concentration may also be related to a positive effect with volume distribution (Dv) increase due to insufficient surfactant to high oil amount (e.g., treatments 3, 4, and 6; Table 1 and Fig. 1G). Concerning Dn 90, the positive effect from EOB concentration in a linear manner may be attributed to the greater substrate (oil) in the nanosystem ($p < 0.05$; Table 2).

Different formulation patterns called “fingerprints” can be observed through the radar chart (Fig. 1G; Bianchin et al., 2015). Some formulations showed a characteristic of uniform monomodal profile distribution. For instance, the formulations with EOB to Tween 80 ratios of 1:4 (e.g., treatments 1 and 2) and 1:1.81 (e.g., treatments 8, 9, 10, and 11) reached uniform distribution profile with sizes inferior or equal to 100 nm (Di 90) and average size less than 25 nm (Di 50). Otherwise, the ratio 1:1 showed Di 90 values > 160 nm and Di 50 > 65 nm (e.g., treatments 3, 4, and 6; Fig. 1G). Previous studies have highlighted that proportions between 1:1 and 1:3 (EO to Tween 80) allow obtaining NEs with sizes < 180 nm (da Silva et al., 2022). However, in the present study, ratios equal to 1:4 or 1:1.81 were promising, achieving smaller droplet sizes (≤ 100 nm).

Da Silva et al. (2023b) reached mean droplet sizes (Di 50) ranging from 54.47 to 84.07 nm, with oregano EO, carvacrol, or thymol at 10 mg/mL, coated with Tween 80 (2.9%; 1:3) and subjected to sonication at 157.5 W for 4.9 min (Power = 13.83 W; AED = 81.3 kJ/mL). Yang et al. (2022) reached NEs with sizes between 16.3 and 17 nm from thyme EO (10 mg/mL) with Tween 80 (10 mg/mL; 1:1) at 350 W during 5 and 15 min (power, ultrasound intensity or AED values were not informed); meantime, size increased

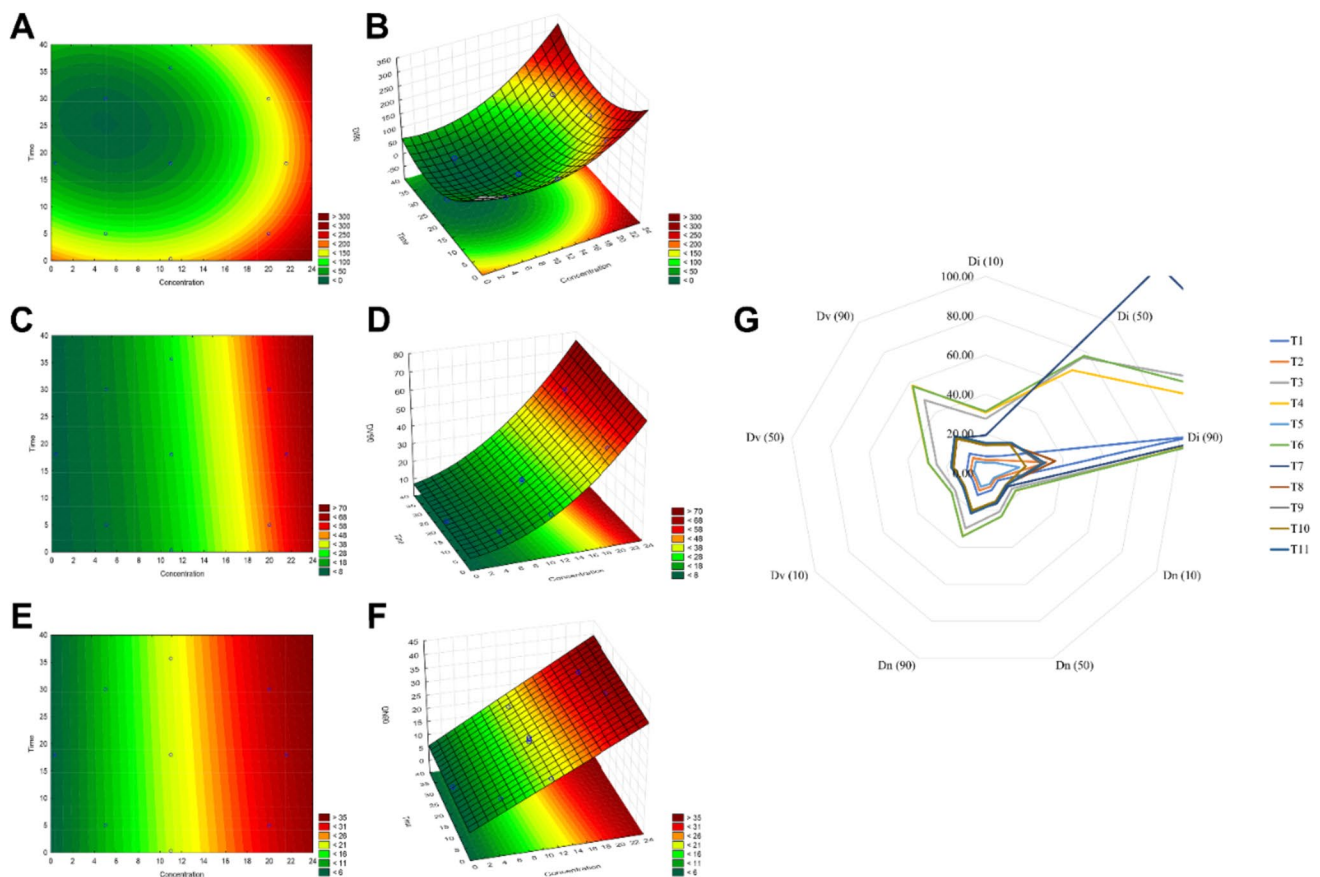


Fig. 1 2D (**A**, **C**, and **E**) and 3D (**B**, **D**, and **F**) surface plots for the effect of ultrasound time exposition and essential oil blend (EOB) concentration on the drop size distribution from 11 experiments generated by central composite rotatable design. **A**, **B** Ninety percent of the population of drops of cumulative intensity (D_i); **C**, **D** 90% of the

population of drops of cumulative volume (D_v); **E**, **F** 90% of the population of drops of cumulative number (D_n); **G** radar chart for D_{10} , D_{50} , and D_{90} values (size of 10%, 50%, and 90% of the population of drops) of cumulative intensity (D_i), volume (D_v), and number (D_n)

together with Tween 80 (20 mg/mL; 1:2), resulting in 47.8 nm. Other studies obtained NE through various coatings, such as Hasheminya and Dehghannya (2022), which used Tween 80 and span 80 as coating, achieved an average droplet size (z -average) of 84.32 nm in a 1:1 ratio of surfactant and EO using ultrasound process. Besides, Hemmatkhan et al. (2020) used Tween 80 to obtain NE from Cumin Seed EO, showing average droplet sizes of 100.3 nm with the same method. Furthermore, lemongrass EO coated with alginate and Tween 80 (1:1:1 ratio) showed different average droplet sizes after being exposed to different sonication times with 34.95 to 5.12 nm, however, showing a multimodal distribution (Salvia-Trujillo et al., 2013). Finally, Xu et al. (2020) reached sizes ranging from 81.67 to 82.09 in obtaining NE with Tween 80 coating cinnamon EO and different concentrations of ascorbic acid (0 to 10 g/L) using the microfluidizer technique. An important fact to be highlighted is that the studies above used only average size data (z -average), not using distribution values by intensity, volume, and number (D_{90} , D_{50} , and D_{10}).

Despite not adjusting to the model (R^2_{adj} , 0.46; LOF, 0.01), the PDI brought important information about the NEOB homogeneity and stability. Briefly, NEs with a monomodal profile on the radar chart showed low PDI values, equal to or less than 0.25 (Supplementary Table 1), except for treatment 5 with the lowest EOB to Tween 80 ratio (1:50) and 7 subjected to the lowest ultrasound time exposure (0.32 min; U.I., 0.76 W/cm² and AED, 0.42 kJ/mL). The PDI is still little studied concerning the variables used in the present study. Nevertheless, it is already been reported that increasing surfactant reduces the PDI to a certain point, wherein it is smaller than 0.25 (da Silva et al., 2022, 2023a) or 0.30 (Pongsumpun et al., 2020) which are indicators of good homogeneity in droplet sizes.

Zeta Potential

The zeta values varied from -3.78 , being able to reach -26 mV. Furthermore, in Fig. 2B, it is possible to observe a sudden increase in the negative charge when (I) the EOB to Tween 80

Table 2 Summarized ANOVA analysis and effect estimates of the significant variables ($p < 0.05$) from central composite rotatable design

Factors ^b	Di 90 ^a		Dv 90		Dn 90	
	EE	SE	EE	SE	EE	SE
Intercept	196.93	8.98	6.90	0.82	5.56	0.52
EOB	-9.70	1.06	-	-	1.26	0.05
Time	-13.70	0.61	-	-	-	-
EOB ²	0.61	0.03	0.08	0.006	-	-
Time ²	0.25	0.01	-	-	-	-
EOB.Time	0.14	0.02	0.01	0.001	-	-
LOF	19.15	-	4.98	-	2.37	-
MSE	27.53	-	0.78	-	0.71	-
R^2_{adj}	0.93	-	0.99	-	0.98	-
Factors	Zeta potential		MIC		FRAP	
	EE	SE	EE	SE	EE	SE
Intercept	-6.77	0.87	3.46	0.16	1.03	0.01
EOB	0.58	0.11	-0.40	0.02	0.01	0.0009
Time	-0.49	0.03	-	-	-0.02	0.001
EOB ²	-0.02	0.004	0.01	0.001	-	-
Time ²	-	-	-	-	0.00076	0.00005
EOB.Time	0.02	0.003	-	-	-	-
LOF	18.99	-	12.48	-	15.36	-
MSE	0.33	-	0.03	-	0.0003	-
R^2_{adj}	0.76	-	0.73	-	0.82	-

MIC minimum inhibitory concentration, *FRAP* ferric-reducing antioxidant power, *EE* effect Estimates, *SE* standard error, *EOB* essential oil blend concentration (mg/mL), *Time* min, *LOF* lack of fit, *MSE* mean square error, R^2_{adj} adjusted R^2 value

^aSize of 10%, 50%, and 90% of the drop population of cumulative intensity (*Di*), volume (*Dv*), and number (*Dn*)

^bOnly the effects and standard deviations of the variables that demonstrated statistical significance are reported

ratio enhanced (EOB concentration reduced) and (II) with the increase of time of exposure to ultrasound. Indeed, this may have been observed mainly with treatments 2, 5, and 8 (Supplementary Table 1).

The surfactant is mainly responsible for the charge of an NE (Raviadaran et al., 2018), and the Tween 80 is a non-ionic surfactant wherein its negative charge is attributed to the presence of residues of its fragmentation by ultrasound (free fatty acids; Ahmed et al., 2012; McClements, 2021; Raviadaran et al., 2018). Therefore, Tween 80 may be fragmented by the increased exposure to ultrasound, causing the release of free fatty acids and thereby changing the surface charge (da Silva, et al., 2023a). It reinforces our suggestion that excess Tween 80 may have influenced the charge reduction (Supplementary Table 1).

In partial agreement with our findings, Yang et al. (2022) reached the highest charge value (-28.7 ± 0.3 mV) in the middle range of Tween 80 with thyme EO (1:1) using a power of 450W by 10 min. Moreover, these authors suggested the sonication time reduction when a high ultrasound power was used to reach higher negative

zeta potential values. Da Silva, et al. (2023a) observed the same behavior using oregano EO, carvacrol, or thymol with Tween 80 at 1:1 and 1:3.5 ratios. However, these authors reached the highest charge (-12.40 ± 0.72 mV) closer to this study by applying ultrasound power of 412 W for 10 min. Moreover, Hemmatkhah et al. (2020), with Tween 80 coating Cumin Seed EO, showed values of -0.3 mV with 200 W for 15 min. In our study, lower zeta potentials (-26 mV; higher negative charge) could be achieved by high ultrasound times and low EOB concentrations (Fig. 2); however, it might not be interesting for antimicrobial and antioxidant activities and, consequently, not for industry.

Anti-Escherichia coli Activity

The ultrasound time exposition (min) did not influence the antimicrobial activity (MIC; $p > 0.05$; Table 2). However, with higher EOB concentration, higher antimicrobial activity (lower MIC) was non-linearly observed ($p < 0.05$). The response surface plots of MIC are depicted in Fig. 3A, B.

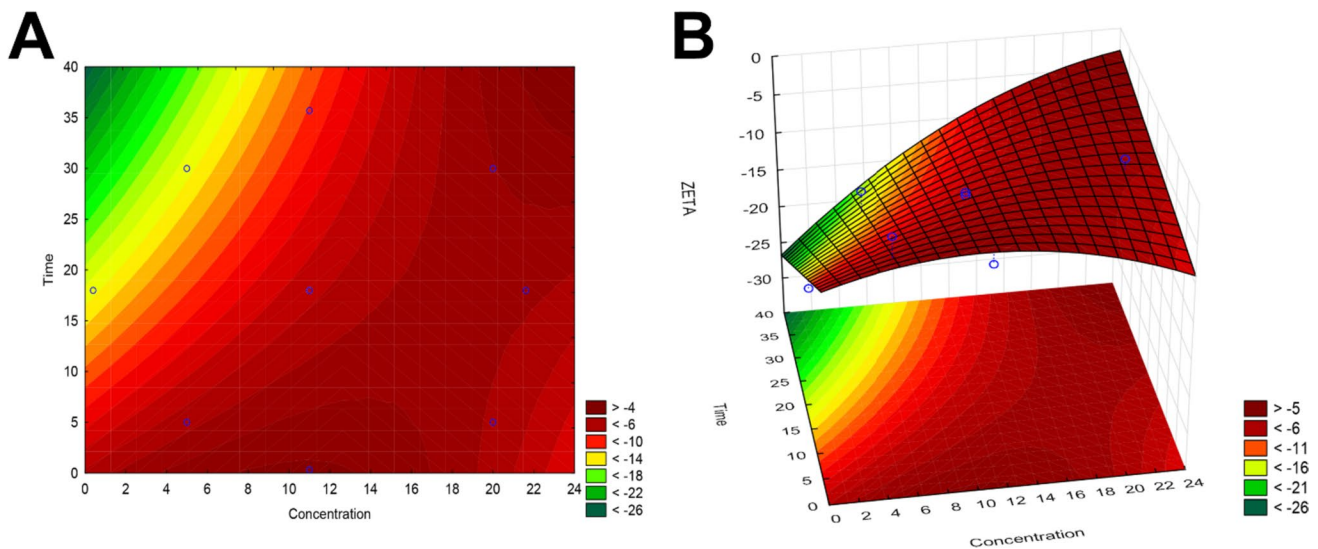


Fig. 2 2D (A) and 3D (B) surface plots for the effect of ultrasound time exposition and essential oil blend (EOB) concentration on zeta potential (mV) from 11 experiments generated by central composite rotatable design

The MIC values ranged from 0.45 to 4 mg/mL, wherein the lowest MIC values were observed in the intermediate concentrations of EOB, emphasizing its non-linear effect (Fig. 3B; Supplementary Table 1).

The NEOB evaluated in this study comprised thyme and lemongrass EOs, which previously showed synergistic potential against *E. coli* (Torres Neto et al., 2022). This synergistic effect was attributed to its composition containing different chemical groups, such as phenols (thymol and carvacrol) and aldehydes (geranial and neral), mainly responsible for antibacterial activity, especially against Gram-negative bacteria. Moreover, due to poor solubilization in water, EOB needs to be coated with an emulsifier, such as Tween 80, that modifies its physical–chemical properties, increasing antimicrobial activity (Jamali et al., 2021).

The emulsifier concentration significantly influences the NE activity since it changes the droplet coating and size distribution (Yang et al., 2022). In the present study, the antimicrobial activity increased as EOB concentration increased (Fig. 3A, B). The antimicrobial effectiveness of EOs has been well-reported in the literature (da Silva, et al., 2023b; Torres Neto et al., 2022). Moreover, the smaller size obtained may have contributed to the increase in antimicrobial activity since intermediate EOB concentrations showed the lowest MIC values (Table S1). The NEs facilitate the entry of EOs through the outer membrane of bacteria due to the nanometric size and hydrophilic groups present in the surfactant, and Tween 80 demonstrates great interaction with the *E. coli* membrane through chemical bond interaction or self-assembly (Majeed et al., 2016; Mushtaq et al., 2023; Sepahvand et al., 2021; Yang et al., 2022). The non-linearity pattern found for MIC values also may be attributed to the influence of the surfactant

amount in releasing oil, wherein the high Tween 80 level (in the case of lower EOB concentration) may form larger micelles encapsulating EOs and impair their actions (Ghazy et al., 2021).

Similarly, da Silva, et al. (2023a) evaluated NEO obtained by ultrasound and observed reduced MIC values for *E. coli*. These authors reported a reduced antimicrobial activity for treatments with high Tween 80 concentration in relation to EO (2.5:1 and 2:1). The same pattern was observed by Yang et al. (2022) using sodium dodecyl sulfate (SDS) and cetylpyridinium chloride (CPC) combined with Tween 80.

Antioxidant Activity

The EOB concentration increased the ferric ion-reducing capacity (FRAP), showing a positive linear effect ($p < 0.05$; Table 2; Fig. 3C, D), and the ultrasound exposition time showed a negative linear and positive quadratic effect. It means high EOB concentrations and low and high ultrasound exposure times (Fig. 3C, D) increased the FRAP. The reduction of the DPPH radical did not fit the model (R^2_{adj} , 0.79; LOF, 0.02), but it was positively correlated with FRAP ($p < 0.05$; Supplementary Table 2).

In short, these results can be explained by the different factors involved in the NE production (e.g., ultrasound time exposition, EOB to Tween 80 ratio, the EO composition, and EO concentration; Cai & Wang, 2021). The relationship between ultrasound's influence on the antioxidant activity in EOs is contradictory in the literature. Jiménez et al. (2018) observed an increase in the antioxidant activity (DPPH) of NE (with sodium alginate together with span 20,

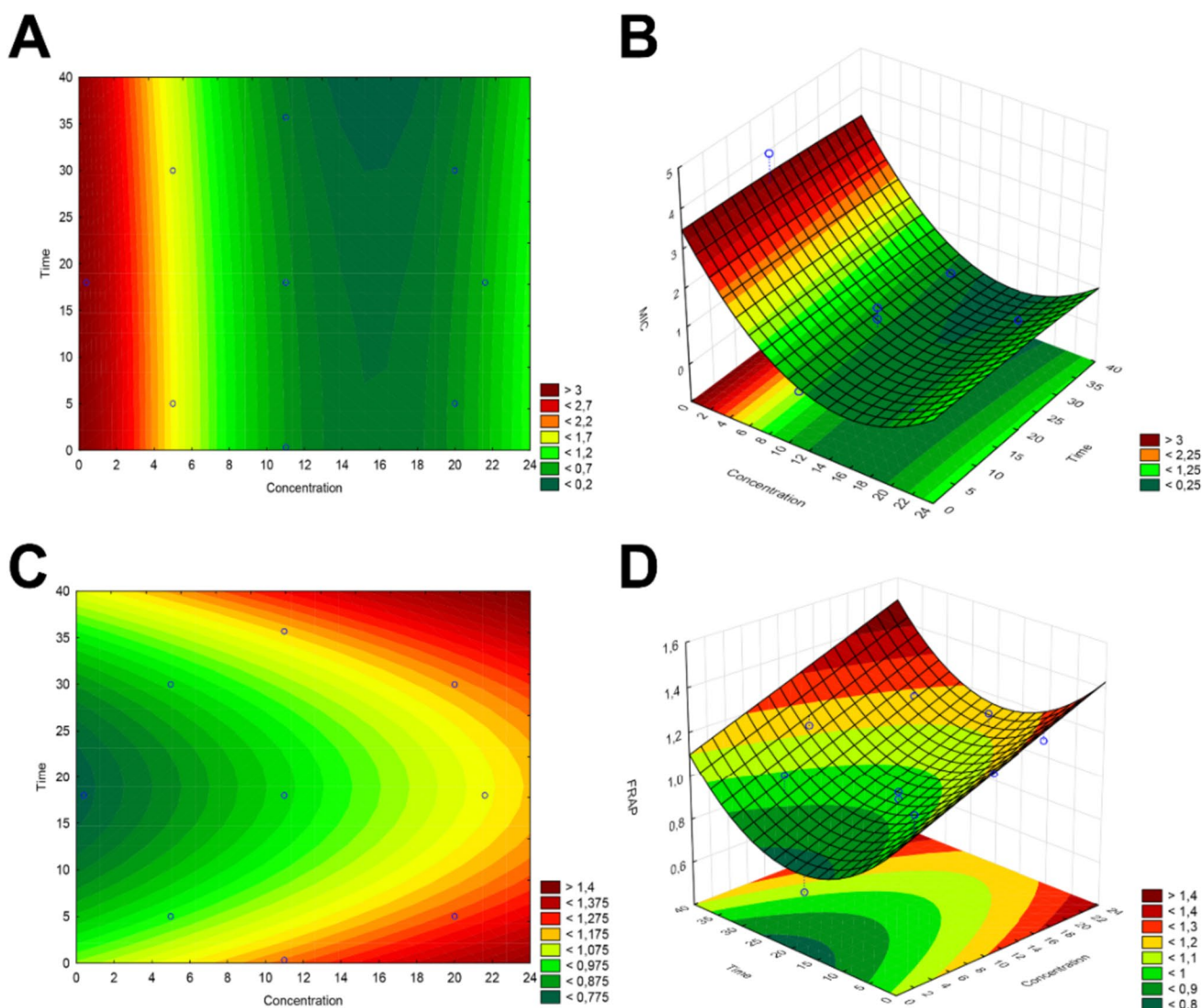


Fig. 3 2D (A, C) and 3D (B, D) surface plots for the effect of ultrasound time exposition and essential oil blend (EOB) concentration on minimum inhibitory concentrations (MIC; A, B) and ferric-reducing

antioxidant power (FRAP; C, D) from 11 experiments generated by central composite rotatable design

hydrophilic-lipophilic balance, Tween 80, Tween 40, and Tween 20 in the formulation) loaded with *C. zeylanicum* EO after the ultrasound process (750 W, 50% duty cycle, and 12 min). This effect was justified by the reduction in the size of the oil droplets, which increased the surface area per unit mass, thus improving the activity of the hydrophobic components. Otherwise, the ultrasound process may also cause oxidative changes in lipids, increasing the amount of free radicals (Jadhav et al., 2023). These facts emphasize the non-linearity observed aforementioned.

Furthermore, Tween 80 can interact with phenols present in EOs through its free hydroxyl groups of the sorbitan moiety (El-Sayed et al., 2017), thereby reducing the antioxidant activity of EOs. Moreover, ultrasound affects lipid portions, releasing free fatty acids, generating variable effects on NEO

depending on EO to Tween 80 ratios (da Silva, et al. 2023a), emphasizing the need to optimize these variables to obtain an effective nanoemulsified system.

The ferric ion-reducing capacity is based on the single electron transfer (SET) mechanism, and the reduction of the DPPH is based on hydrogen atom transfer (HAT) and the SET (Munteanu & Apetrei, 2021; Preedy, 2009). In other words, the SET is specific for antioxidant compounds such as phenols. At the same time, methods with multiple mechanisms of action (e.g., DPPH) include other compounds able to neutralize free radicals through the loss of allylic hydrogen atoms (Olszowy & Dawidowicz, 2016), explaining our findings for FRAP and DPPH.

In this sense, it is possible to infer that HAT activity was little explained by independent variables and their ranges

evaluated in this study. It may be attributed to EOB composition containing 40% of lemongrass, which is composed of high concentrations of geranial and neral (45.5% and 33.7%, respectively), which have an antioxidant mechanism based on HAT (Supplementary Fig. 1; Torres Neto et al., 2022).

Optimization and Validation

It is known that the effects of nanoemulsified EOs with Tween 80 obtained through ultrasound are conflicting in the literature mainly due to the EO composition, EO to surfactant ratio, and ultrasound processing conditions. Therefore, optimizing these variables considering multiple biological activities, such as anti-*Escherichia coli* and antioxidant ones, is crucial to filling gaps in the literature.

The optimal conditions found were 20.518 mg/mL of EOB and 35.677 min of ultrasound (Fig. 4), which resulted in a MIC value for *E. coli* of 0.44 mg/mL and FRAP value of 1.17 μmol TROLOX equivalent/g. It is worth mentioning that the optimal EOB condition to obtain the maximum

anti-*Escherichia coli* and antioxidant activities simultaneously was an EOB to Tween 80 ratio close to 1:1 with the highest EOB concentration. Although this ratio increases the droplet size (Fig. 1G), it directly influences NE bioactivity, wherein Tween 80 reduction decreases the hydrophilic layer and, thus, the surface tension, facilitating the availability of EOB (McClements et al., 2021; Tadros et al., 2004).

The optimal conditions found in this study resulted in an average droplet size value of 68.88 ± 2.84 nm (*Di* 50) and 153.2 ± 10.1 nm (*Di* 90), besides a PDI of 0.287 ± 0.005 . It indicates a nanoemulsion with good stability since coalescence effects can occur at PDI values greater than 0.4, making it unstable (Golfomitsou et al., 2018; Pongsumpun et al., 2020).

The models were externally validated, including three different EOB concentrations (5, 10, and 20.518 mg/mL) combined with an ultrasound time exposition of 35.67 min. In our study, the Af values ranged from 1.66 to 1.38 and Bf values from 1.45 to 1.28, indicating good accuracy of the models (Ross et al., 2000).

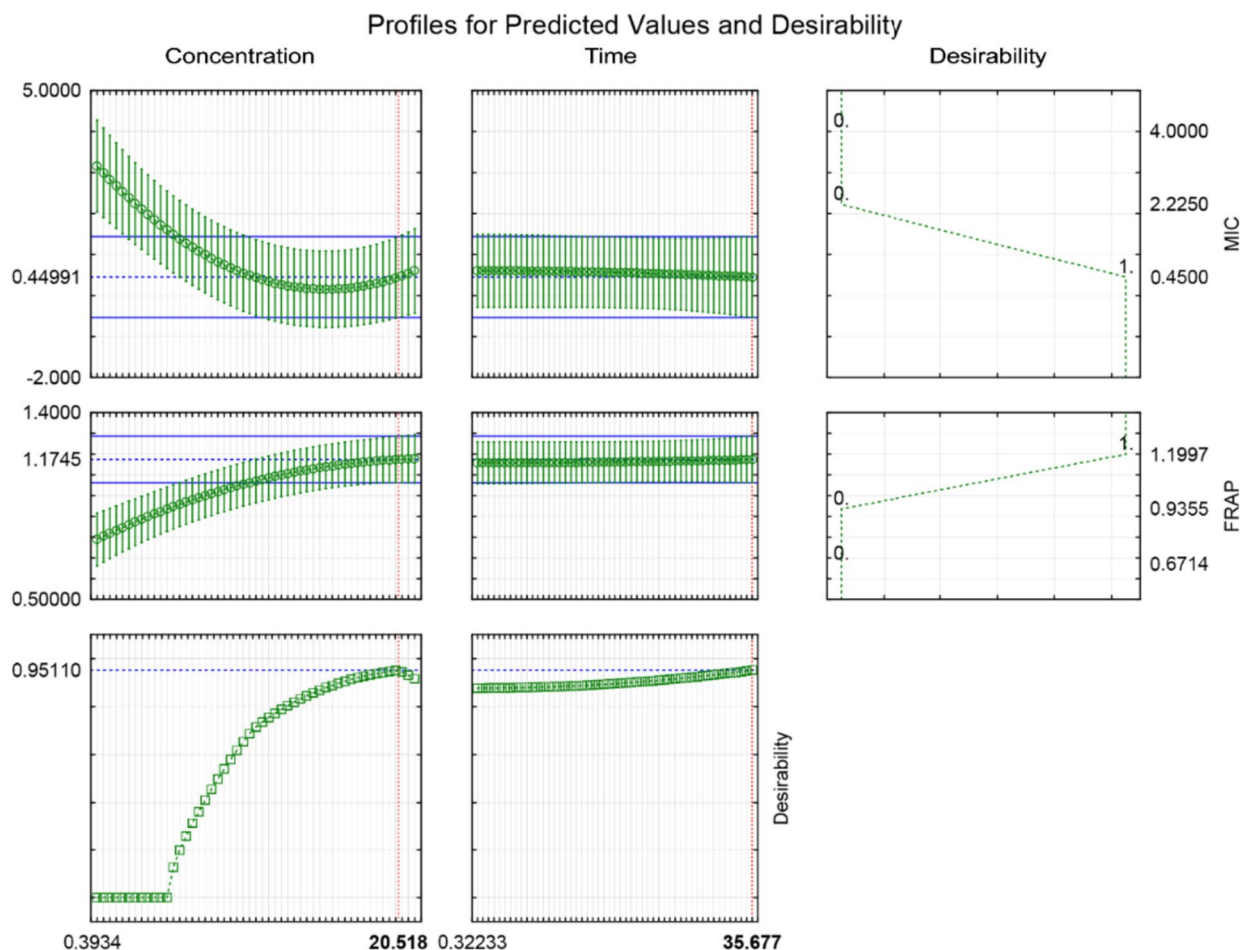


Fig. 4 Desirability plot showing the optimal ultrasound time exposition and essential oil blend (EOB) concentration to achieve the minimum inhibitory concentrations (MIC) and maximum ferric-reducing antioxidant power (FRAP)

UVC-LED Exposure

The NEOBs externally validated were exposed to UVC-LED to observe their oxidative stability. For that, NEOBs at the same EOB concentrations described in the “**Optimization and Validation**” section were prepared, resulting in different EOB to Tween 80 ratios (1:1, 1:2, 1:4), which were submitted to UVC-LED power of 1.78 mW/cm² for 20, 40, and 60 min (2.14 4.27, and 6.41 J/cm², respectively; Fig. 5).

An increase in droplet diameter was observed as the UVC-LED dose increased (Fig. 5A–C), which was more pronounced in *Di* (90), see Fig. 5C. It is interesting to observe that, even at the highest dose (6.41 J/cm²; 60 min), the influence on droplet size was lower in ratios 1:1 (20.518 mg/mL) and 1:2 (10 mg/mL) than in the ratio 1:4 (5 mg/mL; Fig. 5A, B; *Di* 90). In general, the droplet size of the NEOB containing the highest amount of Tween 80 in relation to EOB concentration was more affected, regardless of UVC-LED.

This effect can be attributed to the possible formation of larger micelles (“**Droplet Size and PDI**” section) in NEOB with a higher amount of Tween 80, which can be reinforced by its monomodal distribution (Fig. 5C). Despite that, the highest amount of Tween 80 in relation to EOB concentration showed higher negative values of zeta potential by forming free fatty acids from the Tween 80 degradation induced by ultrasound. Furthermore, our findings may reinforce this explanation, wherein NEOB containing EOB to Tween 80 ratio of 1:4, 1:2, and 1:1 had zeta potential values of -15.45 ± 2.26 , -4.67 ± 1.36 , and -8.00 ± 1.12 , respectively. Moreover, to our knowledge, there are no reports about the influence of oxidation on the size stability of oil-in-water nanoemulsions with Tween 80. However, the protective effect of the EOB against the effects of UVC-LED cannot be ruled out.

Regarding biological activity, different effects were observed (Fig. 5D–F). The ferric ion-reducing capacity decreased with increasing EOB concentration and

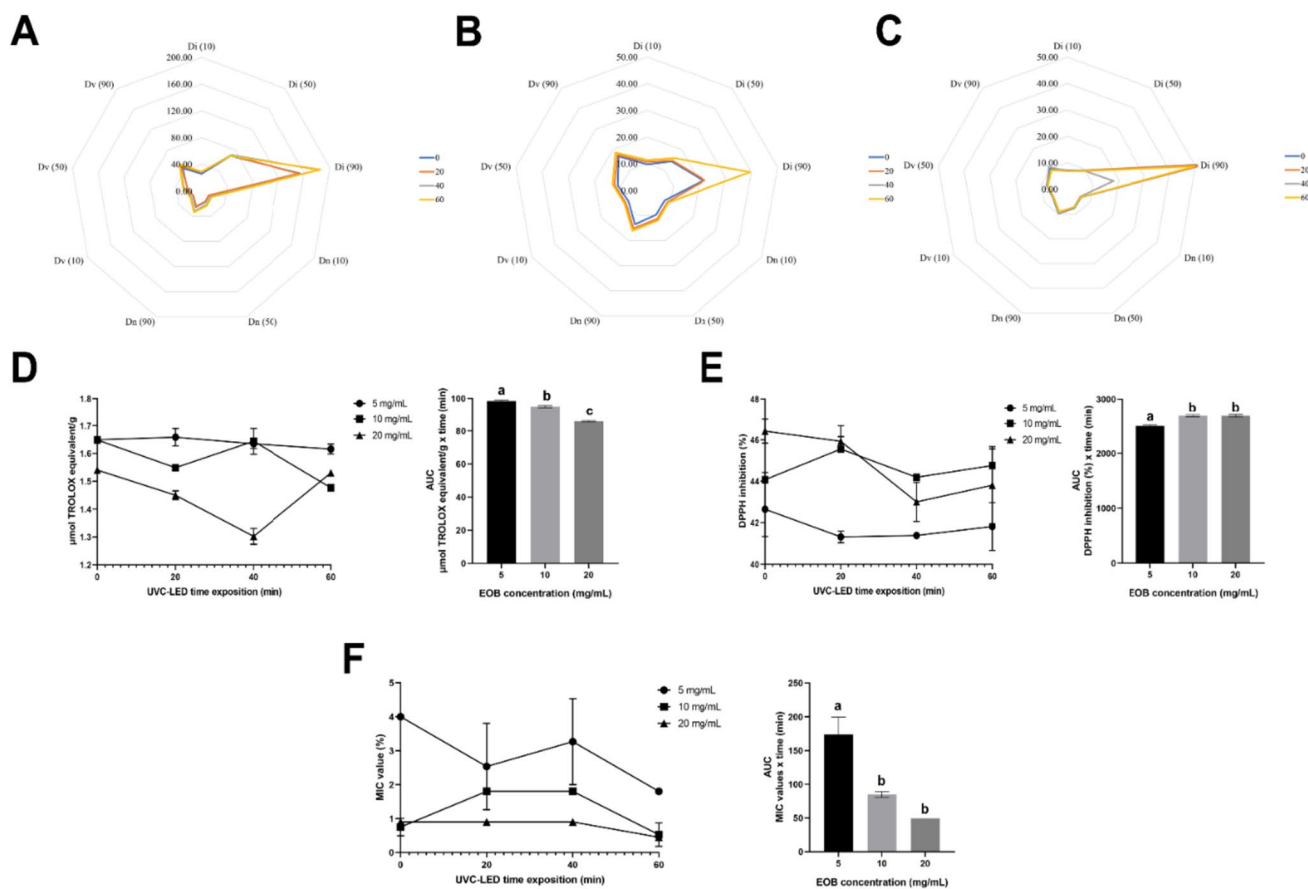


Fig. 5 Radar chart of nanoemulsion loaded essential oil blend (NEOB) at 20.518 (A), 10 (B), and 5 (C) mg/mL exposed to different exposure times of UVC-LED at 1.78 mW/cm², where D10, D50, and D90 values represent size of 10%, 50%, and 90% of the population of drops of cumulative intensity (*Di*), volume (*Dv*), and number (*Dn*); **D** ferric-reducing antioxidant power (FRAP) values during UVC-LED

exposition; **E** DPPH free radical scavenging activity values during UVC-LED exposition; and **F** minimum inhibitory concentrations (MIC) against *Escherichia coli* during UVC-LED exposition. Bars represent average \pm standard deviation ($n=3$). Different letters indicate significant differences ($p<0.05$) among NEOB over exposition

UVC-LED dose, where the formulation with the highest Tween ratio (1:4) provided greater protection to the compounds followed by 1:2 and 1:1 ($p < 0.05$; Fig. 5D). On the other hand, higher amounts of EOB in relation to Tween 80 led to higher DPPH radical inhibition capacity throughout UVC-LED exposure ($p < 0.05$; Fig. 5E). Likewise, the anti-*Escherichia coli* activity remained more elevated in the formulations with the highest EOB concentration in relation to Tween 80 ratio ($p < 0.05$; Fig. 5F).

Despite the protection from phenolic compounds in response to NE exposure to oxidative stress (Fig. 5D; Bayram & Decker, 2023), UVC induces the degradation of these molecules (Wu et al., 2001). Following this hypothesis, this effect can be observed by the reduction of FRAP values when the EOB concentration is higher than Tween 80 ones, generating a NEOB with increased phenol content, which tends to migrate close to the oil/water interface (Ryu et al., 2018), thus, increasing the exposure of the oil core to UVC-LED stress.

On the other hand, phenols maintained certain biological stability of EOB through retaining antioxidant mechanisms (HAT; DPPH) and anti-*Escherichia coli* activity (Fig. 5E, F). Furthermore, greater control was observed with EOB to Tween 80 ratio close to 1:1 during UVC-LED exposure ($p < 0.05$). Thus, the biological activity was maintained even with larger droplet sizes, which may be attributed to the thickness of the surfactant layer, enhancing the release of compounds present in EOB (Tadros et al., 2004).

Conclusion

EOB to Tween 80 ratio and ultrasound exposition time non-dependently affected physical–chemical and biological activity. The optimal biological conditions (the highest anti-*Escherichia coli* and antioxidant activities) were achieved by 20.518 mg/mL of EOB and 35.677 min of ultrasound, which led to a monodisperse formulation with a droplet size below 200 nm. Furthermore, this EOB to Tween 80 ratio close to 1:1 was the most stable concerning biological activity during UVC-LED exposure, even at high doses (6.41 J/cm²). It emphasizes the successful synergistic combination of optimized EOBs and the physicochemical properties of NEs, effectively contributing to further in situ studies and the industrial application of NEOB.

Supplementary Information The online version contains supplementary material available at <https://doi.org/10.1007/s11947-023-03297-6>.

Author Contribution Luiz Torres Neto: conceptualization, formal analysis, data curation, and writing—original draft. Maria Lúcia Guerra Monteiro: conceptualization, formal analysis, data curation, and writing—review and editing. Yhan da Silva Mutz: formal analysis, data curation, and writing—review and editing. Renata Valeriano Tonon: writing—review and editing. Carlos Adam Conte-Junior: funding acquisition, project administration, supervision, and writing—review and editing.

Funding The authors are thankful for the financial support provided by the FAPERJ—grant number [E-26/202.690/2023], [E-26/203.881/2022], [E-26/200.891/2021], [E-26/010.000148/2020], [E-26/201.790/2020], and [E-26/202.710/2019]; the CNPq—grant number [313119/2020–1], [402215/2022–2], and [200468/2022–7]; and the CAPES—grant number [88887.518752/2020–00].

Data Availability Data will be made available on request.

Declarations

Competing Interests The authors declare no competing interests.

References

- Abbas, S., Hayat, K., Karangwa, E., Bashari, M., & Zhang, X. (2013). An overview of ultrasound-assisted food-grade nanoemulsions. *Food Engineering Reviews*, 5(3), 139–157. <https://doi.org/10.1007/s12393-013-9066-3>
- Ahmed, K., Li, Y., McClements, D. J., & Xiao, H. (2012). Nanoemulsion- and emulsion-based delivery systems for curcumin: Encapsulation and release properties. *Food Chemistry*, 132(2), 799–807. <https://doi.org/10.1016/j.foodchem.2011.11.039>
- Alves de Aguiar Bernardo, Y., Kaic Alves do Rosario, D., & Adam Conte-Junior, C. (2023). Ultrasound on milk decontamination: Potential and limitations against foodborne pathogens and spoilage bacteria. *Food Reviews International*, 39(1), 320–333. <https://doi.org/10.1080/87559129.2021.1906696>
- Baj, T., Baryluk, A., & Sieniawska, E. (2018). Application of mixture design for optimum antioxidant activity of mixtures of essential oils from *Ocimum basilicum* L., *Origanum majorana* L. and *Rosmarinus officinalis* L. *Industrial Crops and Products*, 115, 52–61. <https://doi.org/10.1016/j.indcrop.2018.02.006>
- Baj, T., Kowalska, G., Kowalski, R., Szymańska, J., Kai, G., Coutinho, H. D. M., & Sieniawska, E. (2023). Synergistic antioxidant activity of four-component mixture of essential oils: Basil, cedarwood, citronella and thyme for the use as medicinal and food ingredient. *Antioxidants*, 12(3), 577. <https://doi.org/10.3390/antiox12030577>
- Baranyi, J., Pin, C., & Ross, T. (1999). Validating and comparing predictive models. *International Journal of Food Microbiology*, 48(3), 159–166. [https://doi.org/10.1016/S0168-1605\(99\)00035-5](https://doi.org/10.1016/S0168-1605(99)00035-5)
- Bayram, I., & Decker, E. A. (2023). Underlying mechanisms of synergistic antioxidant interactions during lipid oxidation. *Trends in Food Science & Technology*, 133, 219–230. <https://doi.org/10.1016/j.tifs.2023.02.003>
- Benzie, I. F. F., & Strain, J. J. (1996). The ferric reducing ability of plasma (FRAP) as a measure of “antioxidant power”: The FRAP assay. *Analytical Biochemistry*, 239(1), 70–76. <https://doi.org/10.1006/abio.1996.0292>
- Bianchin, M. D., Küllkamp-Guerreiro, I. C., de Oliveira, C. P., Contri, R. V., Guterres, S. S., & Pohlmann, A. R. (2015). Radar charts based on particle sizing as an approach to establish the fingerprints of polymeric nanoparticles in aqueous formulations. *Journal of Drug Delivery Science and Technology*, 30, 180–189. <https://doi.org/10.1016/j.jddst.2015.10.015>
- Cai, L., & Wang, Y. (2021). Physicochemical and antioxidant properties based on fish sarcoplasmic protein/chitosan composite films containing ginger essential oil nanoemulsion. *Food and Bioprocess Technology*, 14(1), 151–163. <https://doi.org/10.1007/s11947-020-02564-0>
- Crespo, Y. A., Bravo Sánchez, L. R., Quintana, Y. G., Cabrera, A. S. T., Bermúdez del Sol, A., & Mayancha, D. M. G. (2019). Evaluation

- of the synergistic effects of antioxidant activity on mixtures of the essential oil from *Apium graveolens* L., *Thymus vulgaris* L. and *Coriandrum sativum* L. using simplex-lattice design. *Heliyon*, 5(6), e01942. <https://doi.org/10.1016/j.heliyon.2019.e01942>
- da Silva, B. D., do Rosario, D. K. A., & Conte-Junior, C. A. (2022). Can droplet size influence antibacterial activity in ultrasound-prepared essential oil nanoemulsions? *Critical Reviews in Food Science and Nutrition*. <https://doi.org/10.1080/10408398.2022.2103089>
- da Silva, B. D., do Rosário, D. K. A., Neto, L. T., Lelis, C. A., & Conte-Junior, C. A. (2023a). Improvement of physicochemical and antibacterial properties of nanoemulsified *origanum vulgare* essential oil through optimization of ultrasound processing variables. *Food and Bioprocess Technology*. <https://doi.org/10.1007/s11947-023-03050-z>
- da Silva, B. D., do Rosário, D. K. A., Neto, L. T., Lelis, C. A., & Conte-Junior, C. A. (2023b). Antioxidant, antibacterial and antibiofilm activity of nanoemulsion-based natural compound delivery systems compared with non-nanoemulsified versions. *Foods*, 12(9), 1901. <https://doi.org/10.3390/foods12091901>
- Delshadi, R., Bahrami, A., Tafti, A. G., Barba, F. J., & Williams, L. L. (2020). Micro and nano-encapsulation of vegetable and essential oils to develop functional food products with improved nutritional profiles. *Trends in Food Science & Technology*, 104, 72–83. <https://doi.org/10.1016/j.tifs.2020.07.004>
- Dinu, M. V., Gradinaru, A. C., Lazar, M. M., Dinu, I. A., Raschip, I. E., Ciocarlan, N., & Aprotosoia, A. C. (2021). Physically cross-linked chitosan/dextrin cryogels entrapping *Thymus vulgaris* essential oil with enhanced mechanical, antioxidant and antifungal properties. *International Journal of Biological Macromolecules*, 184, 898–908. <https://doi.org/10.1016/j.ijbiomac.2021.06.068>
- El-Sayed, H. S., Chizzola, R., Ramadan, A. A., & Edris, A. E. (2017). Chemical composition and antimicrobial activity of garlic essential oils evaluated in organic solvent, emulsifying, and self-microemulsifying water based delivery systems. *Food Chemistry*, 221, 196–204. <https://doi.org/10.1016/j.foodchem.2016.10.052>
- Fadil, M., Fikri-Benbrahim, K., Rachiq, S., Ihssane, B., Lebrazi, S., Chraïbi, M., et al. (2018). Combined treatment of *Thymus vulgaris* L., *Rosmarinus officinalis* L. and *Myrtus communis* L. essential oils against *Salmonella typhimurium*: Optimization of antibacterial activity by mixture design methodology. *European Journal of Pharmaceutics and Biopharmaceutics*, 126, 211–220. <https://doi.org/10.1016/j.ejpb.2017.06.002>
- Future Market Insights. (2023). Clean label ingredients market. *Clean Label Ingredients Market Outlook from 2023 to 2033*. Retrieved September 02, 2023, from <https://www.futuremarketinsights.com/reports/clean-label-ingredients-market>
- Ghazy, O. A., Fouad, M. T., Saleh, H. H., Kholif, A. E., & Morsy, T. A. (2021). Ultrasound-assisted preparation of anise extract nanoemulsion and its bioactivity against different pathogenic bacteria. *Food Chemistry*, 341, 128259. <https://doi.org/10.1016/j.foodchem.2020.128259>
- Golfomitsou, I., Mitsou, E., Xenakis, A., & Papadimitriou, V. (2018). Development of food grade O/W nanoemulsions as carriers of vitamin D for the fortification of emulsion based food matrices: A structural and activity study. *Journal of Molecular Liquids*, 268, 734–742. <https://doi.org/10.1016/j.molliq.2018.07.109>
- Gupta, A., Eral, H. B., Hatton, T. A., & Doyle, P. S. (2016). Nanoemulsions: Formation, properties and applications. *Soft Matter*, 12(11), 2826–2841. <https://doi.org/10.1039/C5SM02958A>
- Hąc-Wydro, K., Flasiński, M., & Romańczuk, K. (2017). Essential oils as food eco-preservatives: Model system studies on the effect of temperature on limonene antibacterial activity. *Food Chemistry*, 235, 127–135. <https://doi.org/10.1016/j.foodchem.2017.05.051>
- Hasheminya, S.-M., & Dehghannya, J. (2022). Development and characterization of *Froriepia subpinnata* (Ledeb.) Baill essential oil and its nanoemulsion using ultrasound. *Food and Bioprocess Technology*, 15(11), 2531–2546. <https://doi.org/10.1007/s11947-022-02899-w>
- Hemmatkhan, F., Zeynali, F., & Almasi, H. (2020). Encapsulated cumin seed essential oil-loaded active papers: Characterization and evaluation of the effect on quality attributes of beef hamburger. *Food and Bioprocess Technology*, 13(3), 533–547. <https://doi.org/10.1007/s11947-020-02418-9>
- Istiqomah, A., Prasetyo, W. E., Firdaus, M., & Kusumaningsih, T. (2022). Valorisation of lemongrass essential oils onto chitosan-starch film for sustainable active packaging: Greatly enhanced antibacterial and antioxidant activity. *International Journal of Biological Macromolecules*, 210, 669–681. <https://doi.org/10.1016/j.ijbiomac.2022.04.223>
- Jadhav, H. B., Gogate, P., & Annature, U. (2023). Analysing the repercussions of ultrasound on triacylglycerols in food. *Food Chemistry Advances*, 2, 100332. <https://doi.org/10.1016/j.focha.2023.100332>
- Jamali, S. N., Assadpour, E., Feng, J., & Jafari, S. M. (2021). Natural antimicrobial-loaded nanoemulsions for the control of food spoilage/pathogenic microorganisms. *Advances in Colloid and Interface Science*, 295, 102504. <https://doi.org/10.1016/j.cis.2021.102504>
- Jiménez, M., Domínguez, J. A., Pascual-Pineda, L. A., Azuara, E., & Beristain, C. I. (2018). Elaboration and characterization of O/W cinnamon (*Cinnamomum zeylanicum*) and black pepper (*Piper nigrum*) emulsions. *Food Hydrocolloids*, 77, 902–910. <https://doi.org/10.1016/j.foodhyd.2017.11.037>
- Kalemba, D., & Kunicka, A. (2003). Antibacterial and antifungal properties of essential oils. *Current Medicinal Chemistry*, 10(10), 813–829. <https://doi.org/10.2174/0929867033457719>
- Khatkar, A. B., Kaur, A., Khatkar, S. K., & Mehta, N. (2018). Characterization of heat-stable whey protein: Impact of ultrasound on rheological, thermal, structural and morphological properties. *Ultrasonics Sonochemistry*, 49, 333–342. <https://doi.org/10.1016/j.ultsonch.2018.08.026>
- Konfo, T. R. C., Djouhou, F. M. C., Koudoro, Y. A., Dahouenon-Ahoussi, E., Avlessi, F., Sohounhloue, C. K. D., & Simal-Gandara, J. (2023). Essential oils as natural antioxidants for the control of food preservation. *Food Chemistry Advances*, 2, 100312. <https://doi.org/10.1016/j.focha.2023.100312>
- Lelis, C. A., Galvan, D., & Conte-Junior, C. A. (2023). Nanocarriers for β -carotene based on milk protein. *Food and Bioprocess Technology*, 16(1), 43–67. <https://doi.org/10.1007/s11947-022-02868-3>
- Majeed, H., Liu, F., Hategekimana, J., Sharif, H. R., Qi, J., Ali, B., et al. (2016). Bactericidal action mechanism of negatively charged food grade clove oil nanoemulsions. *Food Chemistry*, 197, 75–83. <https://doi.org/10.1016/j.foodchem.2015.10.015>
- McClements, D. J. (2012). Nanoemulsions versus microemulsions: Terminology, differences, and similarities. *Soft Matter*, 8(6), 1719–1729. <https://doi.org/10.1039/C2SM06903B>
- McClements, D. J. (2021). Advances in edible nanoemulsions: Digestion, bioavailability, and potential toxicity. *Progress in Lipid Research*, 81, 101081. <https://doi.org/10.1016/j.plipres.2020.101081>
- McClements, D. J., Das, A. K., Dhar, P., & Nanda, P. K. (2021). Nanoemulsion-based technologies for delivering natural plant-based antimicrobials in foods. *Frontiers in Sustainable Food Systems*, 5(February), 1–23. <https://doi.org/10.3389/fsufs.2021.643208>
- Mukurumbira, A. R., Shellie, R. A., Keast, R., Palombo, E. A., & Jadhav, S. R. (2022). Encapsulation of essential oils and their application in antimicrobial active packaging. *Food Control*, 136, 108883. <https://doi.org/10.1016/j.foodcont.2022.108883>
- Munteanu, I. G., & Apetrei, C. (2021). Analytical methods used in determining antioxidant activity: A review. *International Journal of Molecular Sciences*, 22(7), 3380. <https://doi.org/10.3390/ijms22073380>
- Mushtaq, A., Mohd Wani, S., Malik, A. R., Gull, A., Ramniwas, S., Ahmad Nayik, G., et al. (2023). Recent insights into nanoemulsions:

- Their preparation, properties and applications. *Food Chemistry: X*, 18, 100684. <https://doi.org/10.1016/j.fochx.2023.100684>
- Olszowy, M., & Dawidowicz, A. L. (2016). Essential oils as antioxidants: Their evaluation by DPPH, ABTS, FRAP, CUPRAC, and β -carotene bleaching methods. *Monatshefte Für Chemie - Chemical Monthly*, 147(12), 2083–2091. <https://doi.org/10.1007/s00706-016-1837-0>
- Ouedrhiri, W., Balouiri, M., Bouhdid, S., Moja, S., Chahdi, F. O., Taleb, M., & Greche, H. (2016). Mixture design of Origanum compactum, Origanum majorana and Thymus serpyllum essential oils: Optimization of their antibacterial effect. *Industrial Crops and Products*, 89, 1–9. <https://doi.org/10.1016/j.indcrop.2016.04.049>
- Oun, A. A., Bae, A. Y., Shin, G. H., Park, M.-K., & Kim, J. T. (2022). Comparative study of oregano essential oil encapsulated in halloysite nanotubes and diatomaceous earth as antimicrobial and antioxidant composites. *Applied Clay Science*, 224, 106522. <https://doi.org/10.1016/j.clay.2022.106522>
- Paniwnyk, L. (2017). Applications of ultrasound in processing of liquid foods: A review. *Ultrasonics Sonochemistry*, 38, 794–806. <https://doi.org/10.1016/j.ulsonch.2016.12.025>
- Pongsumpun, P., Iwamoto, S., & Siripatrawan, U. (2020). Response surface methodology for optimization of cinnamon essential oil nanoemulsion with improved stability and antifungal activity. *Ultrasonics Sonochemistry*, 60, 104604. <https://doi.org/10.1016/j.ulsonch.2019.05.021>
- Preedy, V. R. (2009). *Beer in health and disease prevention*. In V. R. Preedy (Ed.). Elsevier. <https://doi.org/10.1016/B978-0-12-373891-2.X0001-6>
- Raviadaran, R., Chandran, D., Shin, L. H., & Manickam, S. (2018). Optimization of palm oil in water nano-emulsion with curcumin using microfluidizer and response surface methodology. *LWT*, 96, 58–65. <https://doi.org/10.1016/j.lwt.2018.05.022>
- Ribeiro, A. M., Estevinho, B. N., & Rocha, F. (2021). Preparation and incorporation of functional ingredients in edible films and coatings. *Food and Bioprocess Technology*, 14(2), 209–231. <https://doi.org/10.1007/s11947-020-02528-4>
- Ross, T., Dalgaard, P., & Tienungoon, S. (2000). Predictive modelling of the growth and survival of *Listeria* in fishery products. *International Journal of Food Microbiology*, 62(3), 231–245. [https://doi.org/10.1016/S0168-1605\(00\)00340-8](https://doi.org/10.1016/S0168-1605(00)00340-8)
- Rufino, M. D. S. M., Alves, R. E., de Brito, E. S., de Moraes, S. M., Sampaio, C. D. G., Pérez-Jiménez, J., & Saura-Calixto, F. D. (2006). *Metodologia científica: determinação da atividade antioxidante total em frutas pelo método de redução do ferro (FRAP)*. Fortaleza: Embrapa Agroindústria Tropical. Retrieved May 19, 2023, from <https://ainfo.cnptia.embrapa.br/digital/bitstream/CNPAT-2010/11964/1/cot-125.pdf>.
- Rufino, M. D. S. M., Alves, R. E., de Brito, E. S., de Moraes, S. M., Sampaio, C. D. G., Pérez-Jiménez, J., & Saura-Calixto, F. D. (2007). *Metodologia científica: determinação da atividade antioxidante total em frutas pela captura do radical livre DPPH*. Fortaleza: Embrapa Agroindústria Tropical. Retrieved May 19, 2023, from <https://www.embrapa.br/busca-de-publicacoes/-/publicacao/426953/metodologia-cientifica-determinacao-da-atividade-antioxidante-total-em-frutas-pela-captura-do-radical-livre-dpph>
- Ryu, V., McClements, D. J., Corradini, M. G., & McLandsborough, L. (2018). Effect of ripening inhibitor type on formation, stability, and antimicrobial activity of thyme oil nanoemulsion. *Food Chemistry*, 245, 104–111. <https://doi.org/10.1016/j.foodchem.2017.10.084>
- Salvia-Trujillo, L., Rojas-Graü, A., Soliva-Fortuny, R., & Martín-Belloso, O. (2013). Physicochemical characterization of lemongrass essential oil–alginate nanoemulsions: Effect of ultrasound processing parameters. *Food and Bioprocess Technology*, 6(9), 2439–2446. <https://doi.org/10.1007/s11947-012-0881-y>
- Sepahvand, S., Amiri, S., Radi, M., & Akhavan, H.-R. (2021). Antimicrobial activity of thymol and thymol-nanoemulsion against three food-borne pathogens inoculated in a sausage model. *Food and Bioprocess Technology*, 14(10), 1936–1945. <https://doi.org/10.1007/s11947-021-02689-w>
- Singh, B. K., Tiwari, S., Maurya, A., Das, S., Singh, V. K., & Dubey, N. K. (2023). Chitosan-based nanoencapsulation of *Ocimum americanum* essential oil as safe green preservative against fungi infesting stored millets, aflatoxin B1 contamination, and lipid peroxidation. *Food and Bioprocess Technology*, 16(8), 1851–1872. <https://doi.org/10.1007/s11947-023-03008-1>
- Tadros, T., Izquierdo, P., Esquena, J., & Solans, C. (2004). Formation and stability of nano-emulsions. *Advances in Colloid and Interface Science*, 108–109, 303–318. <https://doi.org/10.1016/j.cis.2003.10.023>
- Tan, S. F., Masoumi, H. R. F., Karjiban, R. A., Stanslas, J., Kirby, B. P., Basri, M., & Basri, H. B. (2016). Ultrasonic emulsification of parenteral valproic acid-loaded nanoemulsion with response surface methodology and evaluation of its stability. *Ultrasonics Sonochemistry*, 29(4), 299–308. <https://doi.org/10.1016/j.ulsonch.2015.09.015>
- Teng, F., He, M., Xu, J., Chen, F., Wu, C., Wang, Z., & Li, Y. (2020). Effect of ultrasonication on the stability and storage of a soy protein isolate-phosphatidylcholine nanoemulsions. *Scientific Reports*, 10(1), 14010. <https://doi.org/10.1038/s41598-020-70462-8>
- Torres Neto, L., Monteiro, M. L. G., Machado, M. A. M., Galvan, D., & Conte Junior, C. A. (2022). An optimization of oregano, thyme, and lemongrass essential oil blend to simultaneous inactivation of relevant foodborne pathogens by simplex–centroid mixture design. *Antibiotics*, 11(11), 1572. <https://doi.org/10.3390/antibiotics11111572>
- Wang, M., Wei, Z., & Zhang, Z. (2023). Antimicrobial edible films for food preservation: Recent advances and future trends. *Food and Bioprocess Technology*. <https://doi.org/10.1007/s11947-023-03178-y>
- Wiegand, I., Hilpert, K., & Hancock, R. E. W. (2008). Agar and broth dilution methods to determine the minimal inhibitory concentration (MIC) of antimicrobial substances. *Nature Protocols*, 3(2), 163–175. <https://doi.org/10.1038/nprot.2007.521>
- Wu, C., Liu, X., Wei, D., Fan, J., & Wang, L. (2001). Photosonolysis degradation of phenol in water. *Water Research*, 35(16), 3927–3933. [https://doi.org/10.1016/S0043-1354\(01\)00133-6](https://doi.org/10.1016/S0043-1354(01)00133-6)
- Xu, J., Zhou, L., Miao, J., Yu, W., Zou, L., Zhou, W., et al. (2020). Effect of cinnamon essential oil nanoemulsion combined with ascorbic acid on enzymatic browning of cloudy apple juice. *Food and Bioprocess Technology*, 13(5), 860–870. <https://doi.org/10.1007/s11947-020-02443-8>
- Yang, Z., He, Q., Ismail, B. B., Hu, Y., & Guo, M. (2022). Ultrasonication induced nano-emulsification of thyme essential oil: Optimization and antibacterial mechanism against *Escherichia coli*. *Food Control*, 133, 108609. <https://doi.org/10.1016/j.foodcont.2021.108609>

Publisher's Note Springer Nature remains neutral with regard to jurisdictional claims in published maps and institutional affiliations.

Springer Nature or its licensor (e.g. a society or other partner) holds exclusive rights to this article under a publishing agreement with the author(s) or other rightsholder(s); author self-archiving of the accepted manuscript version of this article is solely governed by the terms of such publishing agreement and applicable law.